Finite element modelling of damage and failure in fiber reinforced composites

Álvaro Díaz Sáez
Instituto Superior Técnico, Lisboa, Portugal
May 2015

Abstract: Modelling of the damage and failure in fiber reinforced composites through the use of finite element method is the main objective of this dissertation. During the service life of the aircraft, cracks and damages may appear and develop in aeronautical structures, which should be analyzed to determine the decrease of stiffness and resistance due to the presence of the cracks.

Through this work, the behavior of different composite plates with holes are analyzed with Hashin-based damage method and XFEM (eXtended Finite Element Method). The models are validated by comparison with experimental results available in the literature and the computational results obtained with Abaqus are used to compare both methods (criteria). XFEM gives better results because it is capable of detecting the crack growth through the entire laminate, while the Hashin damage method can only predict the first ply failure and damage evolution (but no crack formation is allowed). In addition, the results show, as expected, a higher damage resistance in the plates dominated by 0º plies, since the loads are applied in this direction. Regarding to the different hole radii, it can be appreciated that the plates with smaller holes are stiffer, so they experience higher stresses for the same applied strain, which mean that they damage earlier.

Keywords: Fiber reinforced composites, plates, crack, damage, XFEM, Hashin criterion, finite element method**.**

1 - Introduction

Weight has always been an overriding concern when designing an aircraft. For this reason, different materials have been used throughout history, from simple wood to advanced composite materials. The increasing use of composite materials is due, among other reasons, to their low weight, high stiffness and strength to weight ratios, good fatigue behavior, corrosion resistance and can be constructed to fulfill a predefined strength or performance objective [1, 2]. Making them suitable for its application in the commercial aviation industry. Likewise, composites allow radar signals pass through them, for this reason composites are perfect materials for using wherever radar equipment is operating, both in the air or in the ground. Therefore they have also a great application in the military aircraft industry. There are however some limitations with these materials since they are vulnerable to cracking and interlaminar delaminations. Which can lead to catastrophic failures that affect the security.

Safety should be understood as a necessity, being supported by an extensive and complex certification regulation that forces to measure the aeronautical structures to make sure it supports severe conditions without catastrophic failure. Therefore, the determination of the damage tolerance of the aeronautical structures is one of the targets of the certification processes. All these certification processes involve many efforts and time spent. So the development of models which can predict the onset of the damage and its evolution through the laminate is of great importance in order to reduce the number of tests necessary for the certification of an aeronautical structural element. The ABAQUS [3] commercial FE software is a powerful tool for improving designs and reducing time through the use of the finite element method (FEM) [4].

2 – Damage in composites

2.1 – Failure criteria

The failure mechanism of the advanced composite materials and, therefore, their sensitivity to breakage, durability and

damage tolerance are radically different from those of the metallic materials. General failure is preceded by failure phenomena that happen on a microscopic level such as: matrix microcracking, matrix creep, separation of the matrix/fiber interface, and delamination [5].

There are two main groups of failure criteria in composite materials: (i) failure criteria not associated with failure modes and (ii) failure criteria associated with failure modes [6]. Those of the first group are usually polynomial criteria while the second ones propose different equations depending on the mechanism of breakage. It is important to remark that these failure criteria only predict the first ply failure as a general failure criterion for composite laminates so there is no information about crack evolution either if it fails or if it does not. Within the failure criteria not associated with failure modes they can be highlighted the Tsai-Hill and Tsai-Wu criteria; while regarding to the failure criteria associated with failure modes, there will be reference in this section to the Hashin criterion, since this will be the criterion to be used in the current work.

Apart of the failure criteria, there are degradation models, as for example the "Continuum damage mechanics" and the "Discrete damage mechanics". These models are mathematical representations of the mechanical properties of the material after the damage appears. The part of the "damaged" material will be downloaded redistributing the load between the undamaged material. This process will be repeated until no more load could be supported and then the laminate will have reached the failure. One of the main goals of a degradation model is to correctly characterize the stiffness of the damaged material

2.1.1 – Hashin criterion

Hashin [7] proposed that the criterion to predict the failure of a composite material must necessarily be based on the failure mechanisms of the material instead of being simply an extrapolation of existing criteria for other materials such as it happens in Tsai-Hill and Tsai-Wu criteria. This failure criterion is used for predicting different failure modes as fiber breakage in tension, fiber buckling in compression, matrix cracking and debonding.

Under this idea, the author initially proposed a criterion for a biaxial stress state (Hashin-Rotem, 1973, [8]), and later a second criterion for three-dimensional stress states (Hashin 1980, [7]). The assumptions on which Hashin based his originals proposals are the following ones:

- Separated consideration of the different failure modes:
  - *Fiber failure*: traction and compression.
  - *Matrix failure*: traction and compression.
- The interaction between the different components that are involved in a mode is supposed quadratic.

The expressions of these criteria after making some bi-dimensional simplifications ($\sigma_3 = \tau_{13} = 0$) are shown below, where damage initiation occurs when any of these indexes exceeds "1.0":

Hashin-Rotem criterion, (1973) [8]

- Tensile fiber failure (TFF) $\frac{\sigma_1}{\sigma_{1u}^t} = 1 \quad (\sigma_1 > 0)$ (1)
- Compression fiber failure (CFF) $\frac{|\sigma_1|}{\sigma_{1u}^c} = 1 \quad (\sigma_1 < 0)$ (2)
- Tensile matrix failure (TMF) $\left(\frac{\sigma_2}{\sigma_{2u}^t}\right)^2 + \left(\frac{\tau_{12}}{\tau_{12u}}\right)^2 = 1 \quad (\sigma_2 > 0)$ (3)
- Compression matrix failure (CMF) $\left(\frac{\sigma_2}{\sigma_{2u}^c}\right)^2 + \left(\frac{\tau_{12}}{\tau_{12u}}\right)^2 = 1 \quad (\sigma_2 < 0)$ (4)

Hashin criterion, (1980) [7]

- Tensile fiber failure $\left(\frac{\sigma_1}{\sigma_{1u}^t}\right)^2 + \left(\frac{\tau_{12}}{\tau_{12u}}\right)^2 = 1 \quad (\sigma_1 > 0)$ (5)
- Compression fiber failure $\frac{|\sigma_1|}{\sigma_{1u}^c} = 1 \quad (\sigma_1 < 0)$ (6)
- Tensile matrix failure $\left(\frac{\sigma_2}{\sigma_{2u}^t}\right)^2 + \left(\frac{\tau_{12}}{\tau_{12u}}\right)^2 = 1 \quad (\sigma_2 > 0)$ (7)
- Compression matrix failure $\left(\frac{\sigma_2}{2\tau_{23u}}\right)^2 + \left[\left(\frac{\sigma_{2u}^c}{2\tau_{23u}}\right)^2 - 1\right]\frac{\sigma_2}{\sigma_{2u}^c} + \left(\frac{\tau_{12}}{\tau_{12u}}\right)^2 = 1 \quad (\sigma_2 < 0)$ (8)

where σ_1 is the stress in direction 1, σ_{1u}^t is the ultimate tensile stress in direction 1 (maximum tensile longitudinal strength), σ_{1u}^c is the ultimate compressive stress in direction 1 (maximum compressive longitudinal strength), σ_2 is the stress in direction 2, σ_{2u}^t is the ultimate tensile stress in direction 2 (maximum tensile transversal strength), σ_{2u}^c is the ultimate compressive stress in direction 2 (maximum compressive transversal strength), σ_3 is the stress in

direction 3, τ_{13} is the shear stress in plane 1-3, τ_{23} is the shear stress in plane 2-3, τ_{23u} is the interlaminar ultimate shear strength in plane 2-3 (maximum shear strength in plane 2-3), τ_{12} is the shear stress in plane 1-2, τ_{12u} is the ultimate shear stress in plane 1-2 (maximum shear strength in plane 1-2).

2.2 – eXtended Finite Element Method (XFEM)

The conventional methods for fracture modelling only allow the propagation of the crack along the elements that have been previously predefined. This implies a drawback with damage tolerance problems since it is necessary to define the area where the crack is going to generate and not always it is possible to carry out real experiments of the model to predict where this fact is going to happen. However, thanks to XFEM (eXtended Finite Element Method), used in a finite element software, the mesh is generated regardless of the existence and location of any cracks, so it is not necessary to create any special mesh. The XFEM was first introduced by Belytschko et Black in 1999 [9]. It is an extension of the conventional FEM based on the unity partition concept of Melenk and Babuska (1996) [10], that allows local enrichment functions easily embeddable into a finite element approximation. The original purpose of this XFEM method was the crack analysis, but soon covered other computational applications including modelling fracture, void growth and phase change [2]. Through the XFEM method it is possible to study the onset and propagation of the crack in quasi-static problems. XFEM allows studying the crack growth along an arbitrary path without the need of remeshing the model and it is only available for 3D solid and 2D planar model (Figure 1). Crack can be defined by giving it an initial crack onset or alternatively, the finite element software allows the determination of its location during the analysis, based on the value of the maximum principal stresses calculated in the domain of the crack. Regardless of whether or not is defined the initial location of the crack, the finite element software starts it during the simulation process through the tracking of the regions that suffer principal stress higher than the maximum (allowable) values specified in traction-separation laws [3,10, 11].

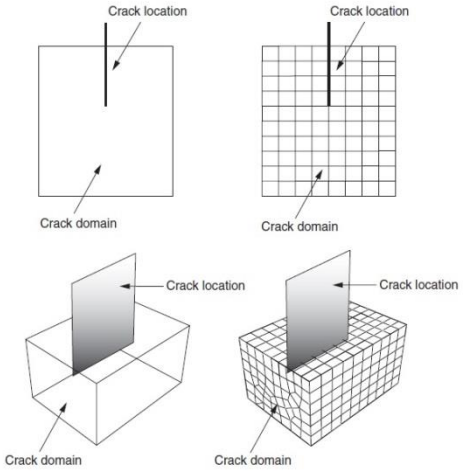

Figure 1. Defining a crack for XFEM [11]

A dynamic crack analysis carried out by XFEM involves two independent parts such as the crack tracking procedure and the dynamic crack propagation formulation. The method used by XFEM is the creation of "dummies" nodes as crack is spreading. The phantom nodes, which overlap with the originals, are introduced to represent the discontinuity of the cracked elements. When the element is intact, each ghost node is completely limited to the corresponding real node. When the element is cut through a crack, cracked element is divided into two parts. Each part consists of a combination of some of the real and phantom nodes depending on the orientation of the crack. Each ghost node and its corresponding real node are not already joined together and can be separated. This system of remeshing is very effective because you can perform more complex crack propagation models since the user does not have to intervene in each analysis increment.

Conventional FEM methods use a piecewise polynomial function that is extended in XFEM with two more extra terms (Equation 9) [11]:

- Heaviside function to represent displacement jump across crack face [$H(x)a_I$; *with I∈ N_T*], where *H(x)* is the Heaviside distribution, a_I is the nodal enrichment degrees of freedom (DOF) vector and N_T the nodes belonging to elements cut by crack.
- Crack tip asymptotic function to model singularity [$\Sigma_1^4 F_\alpha(x) b_I^\alpha$; with *I∈ N_A*], where F_α are the crack tip asymptotic functions and b_I^α the nodal DOF vector.

$$u^k(x) = \Sigma_{I\epsilon N} N_I(x)[u_I + H(x)a_I + \Sigma_1^4 F_\alpha(x) b_I^\alpha] \quad (9)$$

XFEM is capable of analyzing non-linear materials and complex geometries, improving the convergence rates in stationary cracks and defining the onset of the crack with meshing independent of the crack. However, it has some limitations: (i) fatigue crack growth phenomenon cannot be modeled; (ii) a crack cannot turn more than 90 degrees within an element; (iii) crack branching is not allowed; (iv) XFEM is not available in Abaqus/Explicit; (v) only single or non-interacting cracks can be contained in the domain; (vi) parallel processing of elements is not allowed; (vii) only linear continuum elements can be used; (viii) only General Static and Implicit Dynamic analyses can be performed.

3 - Numerical Simulation

A finite element model to investigate the damage and crack of fibre composite plates is shown. The software Abaqus [3] will be used, which will allow doing the necessary analyses to reach the desired objectives of this work. Therefore, a preliminary elastic analysis will be done in order to evaluate the elastic stiffness of the plate and then the damage evolution will be studied throughout the use of both XFEM and Hashin damage criteria.

3.1 - Model Description

The chosen design is a fiberglass laminate (Fiberite/ HyE 9082Af) with a square shape a center hole and nineteen plies (Figure 2). Likewise, the square plate (25x25 mm) has a center hole (1.25 mm radius) that goes through the entire thickness of the plate. Because each ply has a thickness of 0.144 mm, it can be concluded that the plate has a thickness of 2.736 mm.

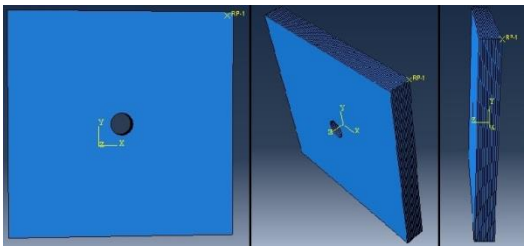

Figure 2. Different views of the square plate

The following table shows the mechanical properties of the composite material used, where the values are given in [1, 12, 13]- see (26) Table 1.

Table 1. Mechanical properties of Fiberite/HyE 9082 Af

Property	Units	Value
Critical energy release rate, mode I, G_{IC}	(kJ/m^2)	0,254
Critical energy release rate, mode II, G_{IIC}	(kJ/m^2)	0,292
Tensile strength in the fiber direction F_{1t}	(MPa)	1020
Compressive strength in the fiber direction F_{1c}	(MPa)	620
Tensile strength in transversal direction F_{2t}	(MPa)	40
Compressive strength in transversal direction F_{2c}	(MPa)	140
Shear strength F_6	(MPa)	60
Transition thickness t_t	(mm)	0,6
Weibull modulus m	-	8,9
Young modulus in the fiber direction E_1	(MPa)	44700
Young modulus in transversal direction E_2	(MPa)	12700
In-plane shear modulus G_{12}	(MPa)	5800
In-plane Poisson's ratio v_{12}	-	0,297
Out-of-plane Poisson's ratio v_{23}	-	0,41
Lamina thickness t_k	(mm)	0,144

Once the problem has been defined, it is possible to mesh the geometry to proceed to the calculation. For the purpose of XFEM analyses, solid (3D) finite elements with label C3D8R were chosen. While for the purpose of Hashin analyses, shell finite elements SC8R were chosen, which belong to the continuum shell elements family. The problem size includes 11420 elements and a total number of variables in the model of 77526 for XFEM and 869 elements and 4316 variables for Hashin-based analyses. The bounday conditions are applied over the left and right sides. In order to fix the plate, all displacements and rotations are restricted on its left side while on the right side the displacements in Y and Z axes directions are the ones fixed. Imposed displacements on the right side of the plate are applied in order to simulate a progressive tensile loading.

3.2 – Validation for stiffness

In order to validate the numerical model developed in the current work, the results were compared with the experimental test results presented by Moure et al. [1]. This way, these results obtained in [1] will be used for making a stiffness validation of the

XFEM and Hashin-based analyses performed in the current work. Figure 3 shows the variation of tensile force with the imposed displacements. It can be concluded that the curve corresponding to XFEM model (red line) matches almost perfectly the experimental test curve (green curve). This means that the elastic stiffness given by the XFEM model is accurate. Regarding the curve provided by Hashin-based analysis (blue curve), it can be concluded that it follow well the XFEM curve for low to moderate load level, but for moderate to high loading it tends to diverge slightly, being the behavior more stiff than the experimental test. Generally speaking, Figure 3 shows a good agreement in the behavior of the three cases. The small differences arise due to different finite elements used, solid elements in case of XFEM and shell in case of Hashin-based analysis.

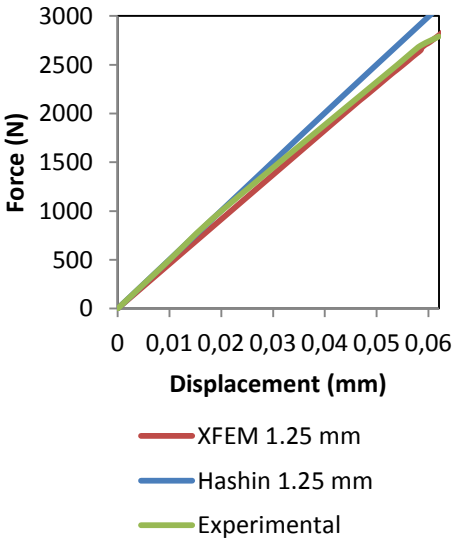

Figure 3. Comparison for the model validation for stiffness

3.3 – Parametric studies

After having validated the model, parametric studies will be shown. Namely, two type of studies will be presented, one related with the different layer configurations and another with different hole radii. Four different types of laminate configurations will be analyzed in order to carry out a parametric study which allows comparing the stiffness properties, the stresses and the forces and displacements when the crack onset appears. These four different stacking sequences are presented in Table 2 where the reference case is the one that appears in [1] and which was used previously to validate the XFEM and Hashin-based models (where subindex "8" means "eight plies"). In all these studies, plates with three different hole radii were considered: one with a hole of 1.25 mm radius, a second one with a 2.50 mm radius hole and finally a third one with a hole of 5.0 mm radius. These studies will be presented separately for XFEM and Hashin-based models.

Table 2. Different stacking sequences

Case	Stacking sequence
Reference Case	$[0, 90_8, 0, 90_8, 0]$
I	$[90, 0_8, 90, 0_8, 90]$
II	$[90_8, 0, 0, 0, 90_8]$
III	$[0_8, 90, 90, 90, 0_8]$

Regarding "Reference Case" and "Case II", most of the layers are 90º oriented, so they will have a low resistance when a tensile load is applied. Therefore, those 90º layers will be the first to fail, followed by the 0º oriented layers. Those layers will support most of the load as they are oriented in the load direction. However, for "Case I" and "Case III", there will be a better overall strength as most of the layers are 0º oriented. For these two cases, failure of 90º layers will take place later, and it will be more progressive. At the end, 0º layers will fail due to overload.

3.3.1- XFEM analyses

When the XFEM analysis is carried out, it can be observed the crack onset and its growth through the entire laminate. For all the studied cases, it can be seen that the crack onset starts around the hole, where the highest stress concentration occurs. When the reference case is analyzed, this failure firstly appears in the 90º plies which transmit the stresses to the central 0º ply resulting also in its failure. After that, the crack still grows perpendicularly to the 0º direction up to the top and the bottom edges. At this point the final failure occurs, taking place the breakage of the two external 0º plies around the central hole and the crack propagation perpendicular to the 0º direction.

Figure 4 illustrates this mode I of fracture after applying a tensile load and the stresses evolution experienced by the composite plate for the "Reference case"

configuration. Green zones show the maximum Von Mises stresses, which are always concentrated on the crack edge.

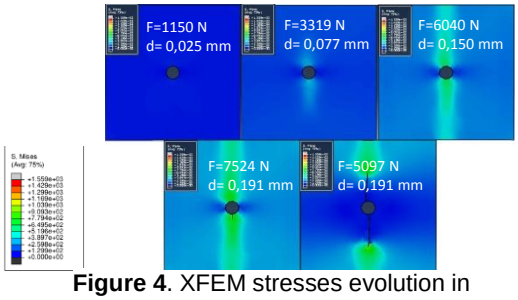

Figure 4. XFEM stresses evolution in "Reference case"

In order to show the material failure and crack propagation in a deeper (zoomed) way, Figure 5 illustrates the studied plate just before and after its final failure.

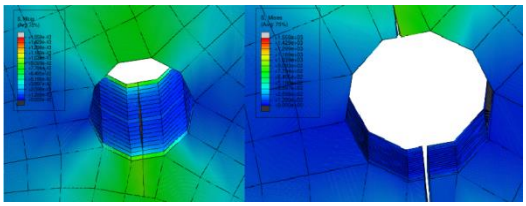

Figure 5. Crack before and after the material failure.

Regarding the plate strength, it can be observed through the Table 4 and Table 6 that "Case I" and "Case III" present the maximum loads (out of four different cases). These two configurations present the maximum number of 0º plies of all the four studied cases, which provides to the laminate a greater resistance in this direction. The same happens for the stiffness, because 0º direction is the direction of application of the imposed stretching displacements (tensile loading). Likewise, as the radius of the hole increases, it can be appreciated a stiffness reduction. The plates with smaller holes are stiffer, so they experience higher stresses for the same applied strain, which mean that they damage earlier. This last statement is verified after checking the following figures and tables: when the radius increases, the displacement at failure is higher and the ultimate load is lower due to the lower net cross-section of the plate.

3.3.2- Hashin-based analyses

In this section, the analysis of the damage suffered by the material is now studied using the Hashin criterion for composites, which predict the first ply failure and damage propagation but no crack formation is allowed (unlike the crack prediction and spread considered by XFEM). As it was said previously, Hashin criterion detects the damage once any of the following failure modes are achieved: (i) fiber tensile failure, (ii) matrix tensile failure, (iii) fiber compressive failure and (iv) matrix compressive failure. In order to detect the damage evolution, the values of the critical energy release rate of the four damage modes are necessary G_{cft} (critical energy release rate for fiber tensile failure), G_{cmt} (critical energy release rate for matrix tensile failure), G_{cfc} (critical energy release rate for fiber compressive failure), G_{cmc} (critical energy release rate for matrix compressive failure), which contrasts with XFEM models where both onset and evolution of damage are predicted in terms of critical ERR only. This is due to fact that the damage addressed by Hashin's method is intralaminar while XFEM analyzes the interlaminar damage through the whole laminate. However, in this work, a first approach was done using the same value of ERR in XFEM for all the four damage modes – this assumption was adopted in order to obtain an equivalent approach between Hashin's method and XFEM [14, 15] and investigate the differences between the ensuing results.

In case of Hashin-based analyses, the evolution of the damage is shown in Figure 6 and Figure 7 for the 0º and 90º plies in "Reference case" for different loading levels. In Figure 6 is possible to appreciate how the damage extends in a perpendicular direction to the applied load for the 0º plies. Figure 7 shows how the damage grows through the entire plate in the 90º plies, due to their low strength regarding the transversal loads.

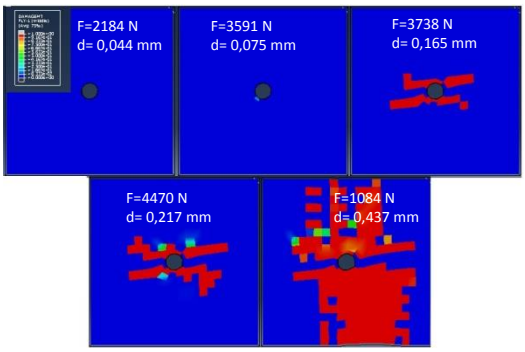

Figure 6. Hashin damage evolution for 0º plies in "Reference case".

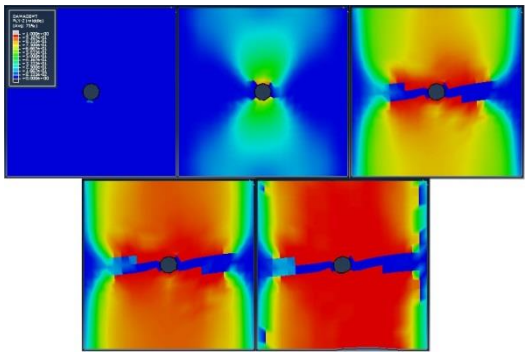

Figure 7. Hashin damage evolution for 90º plies in "Reference case".

Likewise, it is important to show the evolution of different stresses between the 0º and 90º plies that are presented in the laminated plate. The stresses experienced by the 0º plies are higher than those of the 90º plies, which is reasonable after applying a tensile load in 0º direction. The evolution of the stresses for the 0º plies tends to increase in the perpendicular direction to this tensile load, which is consistent with the mode I of fracture that is expected to occur (Figure 8). However, for the 90º plies the stresses tend to grow in the applied load direction due to the fact that these plies are designed to support transverse loads (Figure 9).

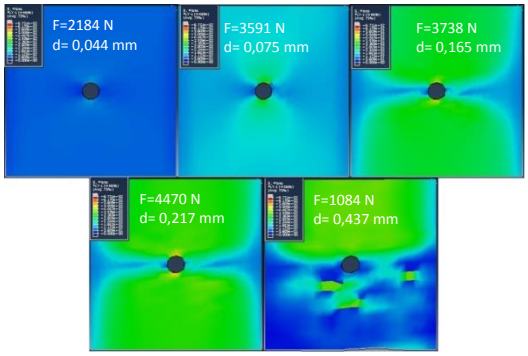

Figure 8. Hashin stresses evolution for 0º plies in “Reference case”

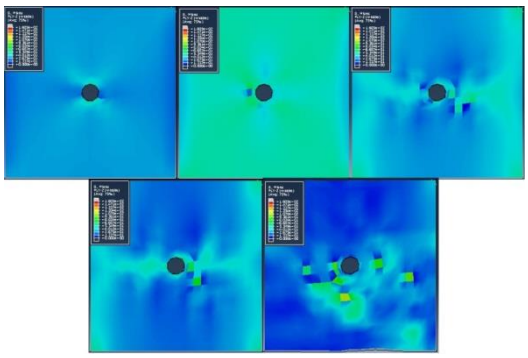

Figure 9. Hashin stresses evolution for 90º plies in "Reference case"

Therefore, based on the obtained results it can be observed that curves of Figures 11 and 13 (“Case I” and “Case III”, respectively) present an almost linear behavior until the maximum load is reached, while those of Figures 10 and 12 (“Reference Case” and “Case II”, respectively) experience a more irregular behavior after the first failure. Additionally, the degradation of stiffness after failure is much more severe in Hashin-based analyses than the crack growth in XFEM analyses.

Likewise, and for all the possible stacking sequences, it can be observed a reduction in the stiffness when increasing the radius hole as it happened in the XFEM cases. In terms of the displacements, it is possible to appreciate how, before the first failure, they are bigger when the radius of the hole increases.
On the other hand, and such it happened when analyzing the plate with the XFEM, the more resistant laminates are those which belong to the Cases I and III since they are the ones that have more plies faced in the direction of application of the imposed displacements (0º direction).

3.3.3 – Comparison between XFEM and Hashin-based results

In this section, a comparison between the XFEM and Hashin-based results will be carried out in order to show the differences that occur when using one of these methods. With this purpose, the curves obtained with both methods for each stacking sequence are overlapped in Figures 10 to 13, while a comparison between the main results of the two methods is gathered in the Tables 3 to 6 (where “H” means Hashin-based method). Also it is necessary to bear in mind that the analyses performed by Hashin’s criterion are based on the assumption of using a similar value of fracture energy for the four failure modes. Regarding the computational efficiency of both methods, the analyses carried out with XFEM took twice the amount of time than the analyses done with Hashin-based method (36000 seconds in average for XFEM and 18000 seconds in average for Hashin-based method). Bearing in mind that the analyses were done using the following processor: “Intel® Core™ i3-2330 M CPU @ 2.20 GHz.

Reference case

For this case, the Figure 10 shows how the values obtained with Hashin are in good agreement with XFEM until the onset of the failure of the first ply. After this point, the force-displacement curves of both methods differ greatly. The differences in the F-d curves for both methods after first failure occur because this "Reference Case" is dominated by the 90º plies and the transversal damage criterion in Hashin was defined in an approximate way (remember that the same value of ERR was used for all the four Hashin damage modes).
As Table 3 shows, the displacements and loads at first failure are very similar for both XFEM and Hashin-based cases. Higher loads at "first failure" are reached with the Hashin –based method while the stiffness values are also in good agreement between the two methods. Very different values of maximum loads are obtained for both methods and a significant reduction in the slopes of the F-d curves could be observed after the first failure for the Hashin-based analyses.

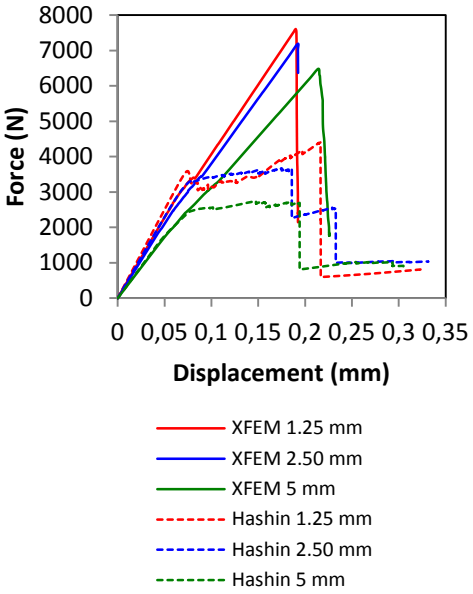

Figure 10. Comparison between XFEM and Hashin-based method for the "Reference case"

Case I

In this case, similar values of force and displacements are obtained with both Hashin and XFEM methods until the ultimate failure, as shown in Figure 11. In this case, the first ply failure follows a more progressive and linear behavior due to the large number of 0º plies which distribute better the stresses between the laminate. As it is shown in Table 4, Hashin-based analyses give higher values of loads and displacements at "first failure" than the values obtained with XFEM, while the stiffness values are very similar for both two methods. Regarding the maximum load, the values of Hashin-based analyses differ approximately ±3000 N from the XFEM values.

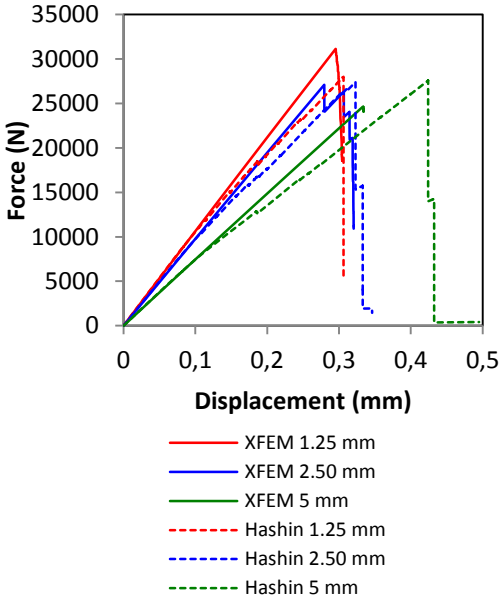

Figure 11. Comparison between XFEM and Hashin-based method for the "Case I"

Case II

For this case, and as it happened in the "Reference case", the Figure 12 shows a similar behavior until the appearance of the "first failure", differing the curves since this point. The differences in the F-d curves for both methods after first failure occur because this "Case II" is dominated by the 90º plies and the transversal damage criterion in Hashin was defined in an approximate way (remember that the same value of ERR was used for all the four Hashin damage modes). When comparing "Reference case" and "Case II" and in spite of the fact that both cases present the same number of 0º and 90º plies, it can be appreciated that "Case II" presents better values of strength than the "Reference case". The three 0º plies stacked together in the midline zone of the laminate (Case II) seems to favor the strength of the laminate.

For both methods, Table 5 shows how the load and displacements values obtained at

"first failure" are almost the same, differing in a small amount. In the same way than in the "Reference case", a very pronounced reduction in the slope of the F-d curves could be observed after the first failure for the Hashin-based analyses.

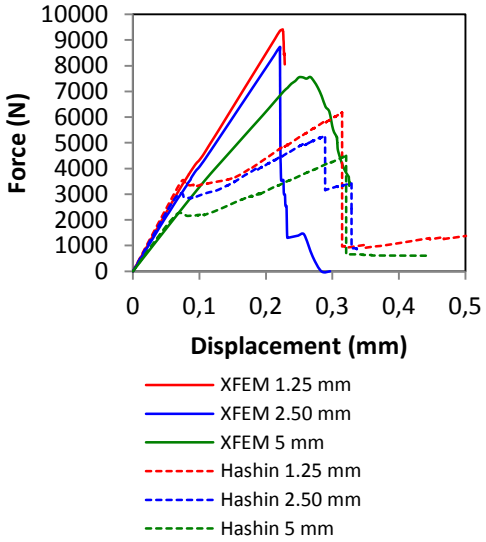

Figure 12. Comparison between XFEM and Hashin-based method for the "Case II"

Case III

The Figure 13 represent a superimposing of the different curves belonging to the analyses did with XFEM and Hashin, showing a similar behavior to the "Case I" previous mentioned. Hashin-based analyses give higher values of loads and displacements at "first failure" than the values obtained with XFEM, while the stiffness values are very similar for both two methods. Regarding the maximum load, the values of Hashin-based analyses differ approximately ±3000 N from the XFEM values-see Table 6.

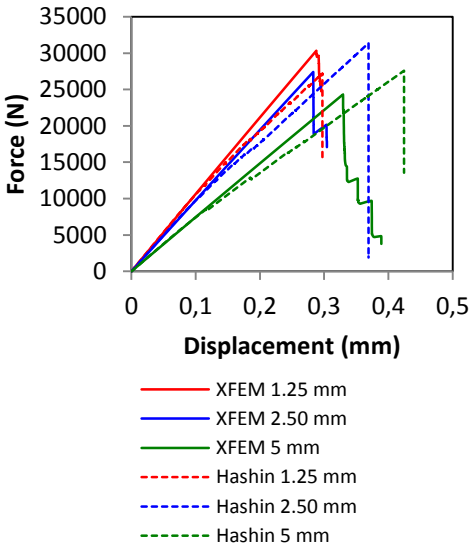

Figure 13. Comparison between XFEM and Hashin method. "Case III".

Table 3. Comparison between XFEM and Hashin-based results for the "Reference case"

	Hole size [mm]					
	1.25		2.5		5.0	
	XFEM	H	XFEM	H	XFEM	H
First failure load [N]	2973	3539	2955	3296	2469	2486
Displacement at first failure [mm]	0,074	0,072	0,074	0,081	0,075	0,082
Maximum load [N]	7524	4407	7191	3641	6485	2695
Displacement at failure [mm]	0,191	0,216	0,192	0,233	0,214	0,194
Stiffness [N/mm]	4,60E+04	5,03E+04	4,28E+04	4,6E+04	3,4E+04	3,6E+04

Table 4. Comparison between XFEM and Hashin-based results for the "Case I"

	Hole size [mm]					
	1.25		2.5		5.0	
	XFEM	H	XFEM	H	XFEM	H
First failure load [N]	13333	14973	12020	14843	11289	12898
Displacement at first failure [mm]	0,125	0,147	0,125	0,161	0,152	0,19
Maximum load [N]	31131	27994	27092	27392	24600	27569
Displacement at failure [mm]	0,295	0,306	0,320	0,323	0,334	0,424
Stiffness [N/mm]	1,1E+05	1,1E+05	9,8E+04	9,9E+04	7,5E+04	7,6E+04

Table 5. Comparison between XFEM and Hashin-based results for the "Case II"

	Hole size [mm]					
	1.25		2.5		5.0	
	XFEM	H	XFEM	H	XFEM	H
First failure load [N]	3177	3510	2920	3033	2608	2273
Displacement at first failure [mm]	0,076	0,073	0,07	0,071	0,079	0,07
Maximum load [N]	9414	6181	8561	5289	7562	4497
Displacement at failure [mm]	0,225	0,311	0,221	0,325	0,266	0,321
Stiffness [N/mm]	4,6E+4	4,9E+4	4,3E+4	4,6E+4	3,3E+4	3,6E+4

Table 6. Comparison between XFEM and Hashin-based results for the "Case III"

	Hole size [mm]					
	1.25		2.5		5.0	
	XFEM	H	XFEM	H	XFEM	H
First failure load [N]	9541	11843	8867	10519	8138	8320
Displacement at first failure [mm]	0,097	0,124	0,091	0,11	0,11	0,121
Maximum load [N]	30314	27168	27407	31369	24312	27582
Displacement at failure [mm]	0,288	0,297	0,304	0,369	0,329	0,424
Stiffness [N/mm]	1,1E+5	1,1E+5	9,8E+4	9,9E+4	7,5E+4	7,6E+4

4 – Conclusions

The aim of this project was the study of the damage and fracture propagation in fiber reinforced composites and its response to a mechanical action. To achieve these purposes, the finite element software Abaqus was used in order to find out the accuracy of different failure criteria when analysing fibre composite laminates made of glass/vinylester. The damage and failure of plates with different radius of the hole and several layer configurations was analyzed through two different methods: (i) eXtended Finite Element Method (XFEM) and (ii) Hashin-based method.

In total, 24 different analyses are done, through XFEM and Hashin-based method, corresponding to plates with three different hole radii (1.25 mm radius; 2.5 mm radius; and 5.0 mm radius) and four different stacking sequences ("Reference case", "Case I", "Case II" and "Case III"). In order to validate the numerical model developed in the current work, a stiffness validation of the XFEM and Hashin-based analyses was made. The results obtained with both methods were compared with the experimental test results presented by Moure et al. [22]. Obtaining good agreement in the behavior of the three cases, with small differences due to the different finite elements used (solid elements in case of XFEM and shell in case of Hashin-based analysis).

Thanks to XFEM, it was possible to detect the onset of cracking and its growth through the entire laminate, providing a complete view of the damage evolution until the final failure of the composite plate is reached. However, the Hashin-based method only predicts the first ply failure and damage propagation but no crack formation is allowed. Resulting the XFEM a much more powerful and accurate method for the study of the fracture propagation in composite materials. However, thanks to Hashin-based method it is possible to obtain a good first approach that allows to study the laminate behavior when it is subjected to a mechanical action. When comparing XFEM and Hashin-based method results, they are in good agreement until the onset of the failure in the first damaged ply, differing the curves above this point. These differences are greater in the "Reference case" and "Case II" than in the "Case I" and "Case III". The laminates dominated by the 0º plies ("Case I" and "Case III") show that the failure of the first damaged ply will take place later and it will be more progressive and slow, so the force-displacement curves for the Hashin-based analyses will be more linear and they will match better with XFEM analyses.

Regarding to the mechanical properties of the different analyzed plates, it is possible to observe that "Case I" and "Case III" are the laminates that present the best strength values. These two configurations present the maximum number of 0º plies of all the four studied cases, which provide the laminate a greater resistance under tensile loading. The same occurs for the stiffness, due to the 0º direction is the direction of application of the imposed stretching displacements (tensile loading). Regarding "Reference Case" and "Case II", most of the layers are 90º oriented, so they have a low resistance when a tensile load is applied. Therefore, those laminates corresponding to the "Reference case" and "Case II" are weaker than the laminated plates in "Case I" and "Case III". Likewise, the hole radius has also a remarkable

importance in the laminate mechanical properties, being able to observe a stiffness reduction as the hole radius increases. The plates with smaller holes are stiffer, experiencing higher stresses for the same applied strain, which leads to an earlier failure.

When comparing “Reference case” and “Case II” and in spite of the fact that both cases present the same number of 0º and 90º plies, it can be appreciated that “Case II” presents better values of strength than the “Reference case”. The three 0º plies stacked together in the midline zone of the laminate (Case II) seems to favor the strength of the laminate. Conversely, the same three plies stacked separately lead to lower strength of the laminated plate because they are connected through 90º layers that weaken the resistance of the group. The stiffness is very similar but the strength profit is better using [90_8, 0, 0, 0, 90_8] rather than [0, 90_8, 0, 90_8, 0]. However, when comparing “Case I” and “Case III”, it can be observed that the large number of 0º plies being placed together cause that the position of the only three 90º plies has not a decisive impact in the results. Regarding the computational efficiency of both methods, the analyses carried out with XFEM took twice the amount of time than the analyses done with Hashin-based method. This is largely due to the high difference in the number of elements and variables used in XFEM (11420 elements and 77526 variables) and in Hashin-based method (869 elements and 4316 variables).

References

[1] M. M. Moure, S. Sanchez-Saez, E. Barbero, E. J. Barbero, “Analysis of damage localization in composite laminates using a discrete damage model”, Composites: Part B, 66, 224-232, (2014).

[2] D. Motamedi, S. Mohammadi, “Fracture analysis of composites by time independent moving-crack orthotropic XFEM”, International Journal of Mechanical Sciences, 54, 20-37, (2012).

[3] Simulia, “Abaqus/CAE”, version 6.10, 2010. User’s manual.

[4] Z. M Huang, ”Failure analysis of laminated structures by FEM based on nonlinear constitutive relationship”, Composites Structures, 77, No. 3, 270-279, (2007).

[5] A. Fernandez, A. Guemes, J. M. Menéndez, J. Mª Pintado, “Materiales Compuestos (CTA-VA)”, Escuela de Ingeniería aeronáutica y del Espacio, Universidad Politécnica de Madrid, Madrid, Spain (2013).

[6] F. Paris, "A study of failure criteria of fibrous composite materials", NASA/CR-2001-210661, (2001).

[7] Z. Hashin, “Failure criteria for unidirectional fiber composites”, Journal of Applied Mechanics, 47, 329-334, (1980).

[8] Z. Hashin, A. Rotem, "A fatigue failure criterion for fiber reinforced materials", Journal of Composite Materials, 7, 7448-7464, (1973).

[9] T. Belytschko, T. Black, “Elastic crack growth in finite elements with minimal remeshing”, International Journal of Numerical Methods in Engineering, 45, 601-620, (1999).

[10] J. M. Melenk, I. Babuska, “The partition of unity finite element method: basic theory and applications”, Computational Methods Applied in Mechanics and Engineering, 139, 289-314, (1996).

[11] Z. Z Du, “eXtended Finite Element Method (XFEM) in Abaqus. Dassault Systémes”.

[12] E. J. Barbero, “Introduction to composite materials design”, 2nd ed. Philadelphia, PA: CRC PRESS, (2011).

[13] E. J. Barbero, F. A. Cosso, X. Martinez, “Identification of fracture toughness for discrete damage mechanics analysis of glass-epoxy laminates”, Applied Composite Materials, 1-18, (2013).

[14] E. J. Barbero, F. A. Cosso, R. Roman, T. L. Weadon, “ Determination of material parameters for Abaqus progressive damage analysis of E-glass epoxy laminates”, Composites Part B, 46, 211–220, (2013).

[15] A. M. Girao Coelho, J. T. Mottram, K. A. Harries, ”Finite element guidelines for simulation of fibre-tension dominated failures in composite materials validated by case studies”, Composite Structures 126, 299-313, (2015).